 DOI: 10.1002/masy.201150315

Polypropylene Nanocomposites, Study of the Influence of the Nanofiller Nature on Morphology and Material Properties

D. Tabuani,[*1] *S. Ceccia,*[2] *G. Camino*[2]

Summary: In this paper we investigate the influence of various nanofilllers' aspect ratio, chemical nature and organic modification on some selected polypropylene properties, such as crystallinity, thermal and mechanical resistance and fire behaviour. Materials were prepared by twin-screw extrusion and characterized by means of scanning electron microscopy, X-ray diffraction, thermogravimetric analysis, tensile and cone calorimeter tests. Fillers characteristics were found to influence at different extents, and for different reasons, the material final properties.

Keywords: extrusion; fire behaviour; mechanical properties; nanocomposites; thermal properties

Introduction

In recent years great attention has been devoted from the polymer materials research community to the study of the characteristics of nanocomposites, especially for what concerns the understanding of the factors leading to the desired dispersion (*nanodispersion*) influencing the final material properties.

In particular, researchers have focused their attention on layered silicates (*nanoclays*) addressing all the possible issues related to the preparation of nanocomposites.[1–4] The addition of nanoclays to a polymer matrix was proven to bring unambiguous advantages in terms of improved mechanical properties, thermal stability, fire resistance, gas barrier, etc.[1,2]

Along the past decades, other kinds of fillers, differing one from the other from chemical and structural point of view, have raised researchers' attention. Reports can be found in the literature concerning for example carbon nanotubes,[5] polyhedral oligomeric silsesquioxanes,[6] boehmites,[7,8] layered double hydroxides,[9] all concerning the dispersion of such fillers in a given polymer and/or evaluating their influence on the material final properties.

Nanofillers can be in general grouped based on their aspect ratio, which is related to their shape factor, as lamellar, tubular or sphere-like; moreover, a key factor characterizing these materials is the possibility to modify them with organic tails in order to make them more compatible with the polymer matrices. Both these aspects can strongly influence the polymer/filler interactions and consequently the material final properties.

As far as polypropylene based materials are concerned, extensive work has been done quite recently evaluating the influence of the compatibiliser (typically polypropylene-grafted maleic anhydride, PPgMA)/clay ratio on the structure and properties of the final materials.[10] The clay aspect ratio was also taken in to account by other authors considering its influence on the melt extensional properties.[11] Dong et al. evaluated the effects of clay type, compatibiliser/clay content and matrix viscosity on the mechanical properties of polypropylene/organoclay nanocomposites.[12] It is

[1] Consorzio PROPLAST, Strada Comunale Savonesa 9, 15057 Alessandria, Italy
Fax: +3901311859789;
E-mail: daniela.tabuani@proplast.it
[2] Politecnico di Torino, sede di Alessandria, Viale T. Michel 5, 15100 Alessandria, Italy

anyway worth noticing that the great majority of the literature reports are dealing, as far as layered silicate are concerned, with the variation of the interlayer cation chemical nature.[1]

When considering natural fillers other than layered silicates only one report can be found in the literature concerning the influence of filler/polymer interaction on the material final properties: recently Bilotti et al. have indeed evaluated the influence of the addition of different functionalized polymers on the dispersion of sepiolites in PP and on the final material crystallinity and mechanical properties.[13]

Up to now no reports are present in the literature which address a comprehensive study of the influence of the filler aspect ratio and chemical nature on PP nanocomposites properties.

In this paper we want to evaluate the influence of different nanofillers, characterized by various aspect ratios as well as organic modification, on polypropylene mechanical, thermal and fire properties also establishing a relationship with the obtained nanomaterial structure. The comparative studies were exploited keeping the same inorganic load for all fillers (5 wt.%) in order to better evaluate the possible influence of the different chemical natures.

Materials and Methods

Polypropylene (PP) was a Basell Moplen HP500N. As far as layered materials are concerned, we addressed two kinds of system: a natural constituted by organically modified Al/Mg phyllosilicates (montmorillonite – characterised by negative charged lamellae) and a synthetic one composed by a modified layered double hydroxide (hydrotalcite – characterised by positive charged lamellae). The montmorillonite was exchanged with a dimethyl dihydrogenated tallow ammonium, whereas the hydrotalcite with a C16-C18 fatty acid. We also took into account needle-like (magnesium hydrosilicate, sepiolite, needle size: 100–500 nm length and 8–20 nm width) and cubic fillers (aluminum oxide hydroxide, boehmite, primary particle size 500–700 nm) both in their pristine forms. Nanofillers characteristics and suppliers are listed in Table 1.

The material containing montmorillonite was prepared with the addition of a polypropylene-grafted-maleic anhydride (PPgMA, Polybond 3200 from Chemtura, USA) as compatibiliser at 5 wt.%.

Before processing nanofillers were dried 4 hours at 100 °C under vacuum.

PP nanocomposites were prepared by using a Leistritz ZSE 27 mm L/D 40 co-rotating intermeshing twin screw extruder (Figure 1). The screw speed was 230 rpm and the temperature of the extruder was maintained at 220 and 200 °C from hopper to dye, respectively. Nanofillers were fed from side-feeder and neat PP was submitted to identical processing to ensure the same thermomechanical history.

The composition, which correspond to a 5 wt.% inorganic content (as determined by

Table 1.
Nanofillers characteristics.

Nanofiller code	Nanofiller type	Organic modifier	Supplier	Filler shape factor
C20A	Montmorillonite	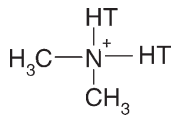	Southern Clay, USA	Layer
F100	Hydrotalcite	C16-C18 Fatty acid	Akzo Nobel, The Netherlands	Layer
CD1	Sepiolite	None	Tolsa, Spain	Needle
Disperal	Boehmite	None	Sasol, Germany	Cubic

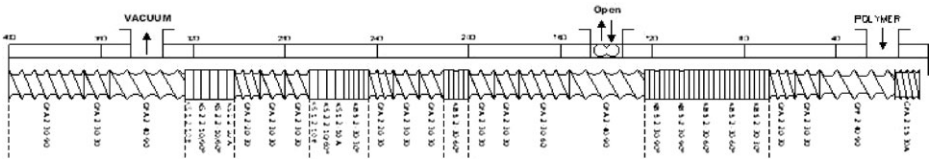

Figure 1.
Screw profile used for the preparation of nancomposites.

TGA analyses, not reported here), of the prepared materials is reported in Table 2.

The extrudates were injection moulded to standard dog-bone shaped tensile specimens for tensile tests according to ISO527-2 (1A) and further characterizations and to $100 \times 100 \times 6\,mm^3$ plaques for fire performance testing.

X-Ray (WAXRD) diffraction patterns were obtained on a ARL XTRA48 diffractometer using Cu Kα radiation (λ = 1,54062 Å). Radial scans were recorded in the reflection scanning mode from 2θ = 5–25° for PP, step-size 0.02° at 2°/min scanning rate.

Scanning Electron Microscopy (SEM) imaging was performed on a LEO 1450 VP instrument on gold sputtered cryogenic fracture surfaces.

Transmission electron microscopy (TEM) were performed with a FEI TECNAI 100 instrument (accelerated voltage: 100 kV); the samples were cut using a Leica ultracryomicrotome apparatus, obtaining sections of 100–200 nm thickness.

Differential Scanning Calorimetry (DSC) analyses were run using a TA Q1000 instrument in hermetic aluminium pans, under nitrogen flow (50 ml/min). Heating rate was 10 °C/min from 25 to 300 °C performing three successive runs (heating-cooling-heating), on ca. 4 mg samples. The crystallisation (T_c) and melting (T_m) temperatures were evaluated as the maximum of the crystallisation and melting peaks, respectively, with a ±0.5 °C tolerance and the degree of crystallization was calculated from the peak enthalpy area normalized to the actual polymer weight fraction according to:

$$X_C = \frac{\Delta H_m}{\Delta H_m^0 \times W_{polymer}} \times 100$$

where ΔH_m is the melting enthalpy (calculated as the area under the melting peak), ΔH°_m is the theoretical melting enthalpy for PP (equal to 165 J/g[14]) and $W_{polymer}$ is the polymer mass fraction. Values were derived from single DSC analyses for each sample. Thermogravimetry (TGA) was performed on a TA Q 500 instrument, on ca. 10 mg samples (from extruded material), in Platinum pans, with gas fluxes of 60 ml/min for sample gas (nitrogen or air), and 40 ml/min for balance protection gas (nitrogen) heating at 10 °C/min between 50 and 800 °C. $T_{5\%}$ was defined as the temperature at 5% of weight loss and T_{max} as the maximum weight loss rate temperature (*i.e.* derivative TGA, peak temperature). $T_{5\%}$ and T_{max} were measured within a ±3 °C tolerance on single runs.

Combustion tests were performed on a Fire Testing Technology Cone Calorimeter according to ISO 5660, on $100 \times 100 \times 6\,mm^3$ specimens, prepared by injection moulding. Tests were performed at $50\,kW/m^2$ external heat flux, in order to evaluate the fire properties of the composites in conditions comparable to a developing fire scenario;[15] specimens were wrapped in an aluminium foil leaving the upper surface exposed to the radiator and

Table 2.
Sample composition.

Samples	Composition (wt%)
PP	100
PP/F100	90/10
PP/CD1	95/5
PP/Disperal	95/5
PP/PPgMA	95/5
PP/ PPgMA /C20A	87.3/5/7.7

placed on ceramic backing board at a distance of 25 mm from the heating cone base. Three tests for each sample were performed and in the following section the average values will be discussed.

Tensile tests were performed according to the UNI EN ISO 527 on a Zwick Roell Z010 testing machine with crosshead speed of 50 mm/min. The data reported represent the average of at least 10 successful tests. The experimental error was ±3% for E, and ±25% for ε_b. Samples were put under vacuum after injection moulding and kept in the same conditions until testing.

Results and Discussion

Morphology

Structural characteristics of the prepared samples were assessed through SEM and XRD analysis.

Figure 2 shows SEM micrographs obtained for each sample.

Both layered materials display a quite good compatibility with the polymer matrix, as we can observe on the fracture surface the presence of well distributed small residual aggregates (Figure 2a and 2b).

It is also worth noticing that sepiolite CD1, despite being completely inorganic, shows a good level of interaction with PP with a good distribution of small aggregates, even though some large residual aggregates can be identified (Figure 2c) in the micrograph.

Disperal, on the other hand, presents a very poor compatibility with the matrix with very large (ca. 40 μm) residual aggregates on the fracture surface (Figure 2d) whereas Disperal primary particle size is 500–700 nm.

The dispersion of the fillers in the matrix was determined by XRD, with the exception of CD1 and Disperal whose XRD pattern, being these non swelling materials, is not influenced by their dispersion in polymers.

Despite the good level of distribution, a very poor degree of dispersion is observed through XRD analysis for C20A. Indeed the main diffraction peak of the pristine material, centred at 2θ 3.7 (corresponding

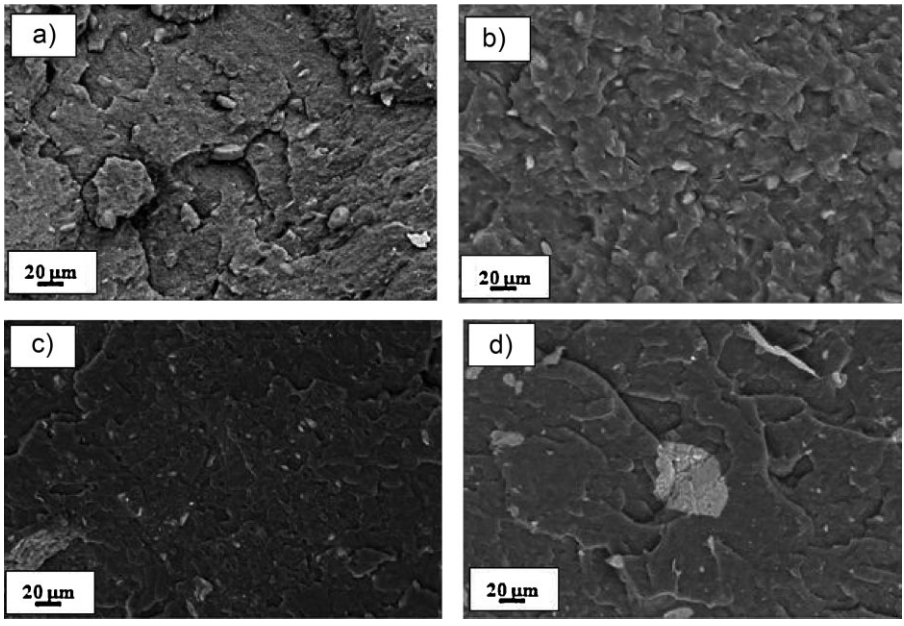

Figure 2.
SEM micrographs nanocomposites: PP + C20A (a), PP + F100 (b), PP + CD1 (c), PP + Disperal (d).

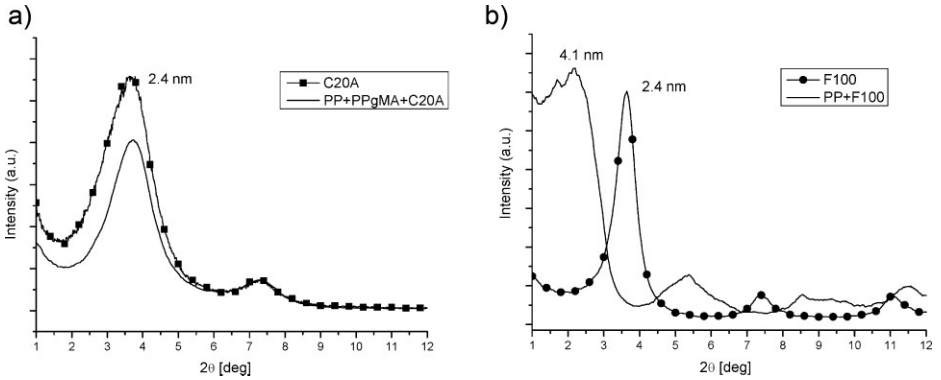

Figure 3.
XRD spectra of organoclay nanocomposites based on C20A (a) and F100 (b).

to an interlayer distance of 2.4 nm) is not shifted after processing with PP.

To further investigate C20A dispersion and to understand better the important properties improvements observed upon the addition of this clay (*vide infra*), TEM analyses were performed, which reveal a complex morphology ranging from micro-composite (due to the presence of large residual aggregates) to a partially exfoliated structure with small tactoids distributed in the polymer matrix (Figure 4b).

The difference with the morphology derived from XRD analysis (microcomposite) may be attributed to a variation of clay dispersion from nano to microcomposite going from the inner core (TEM/SEM) to the outer layer (XRD) of the injection moulded specimen, as already pointed out by Lee et al for a thermoplastic polyolefin based material.[16]

F100 based system shows an intercalated structure as the main diffraction peak, located at 2θ 3.7 for the pristine material, is shifted to 2θ 2.2 after processing, with an increase of the interlayer distance of 1.7 nm (from 2.4 to 4.1 nm). This result gains even more prominence considering that the material containing F100 was prepared without any compatibiliser. It is therefore likely that the negatively charged organic modifier of F100 creates a chemical environment more suitable to the insertion of PP chains in between the layers. It is worth noticing that the initial interlayer distance of both clays is the same and therefore the reason of a higher interaction has to be found in the chemical nature of the clay galleries. Indeed organically modified hydrotalcites are known to exfoliate in polyolefins, such as polyethylene.[17]

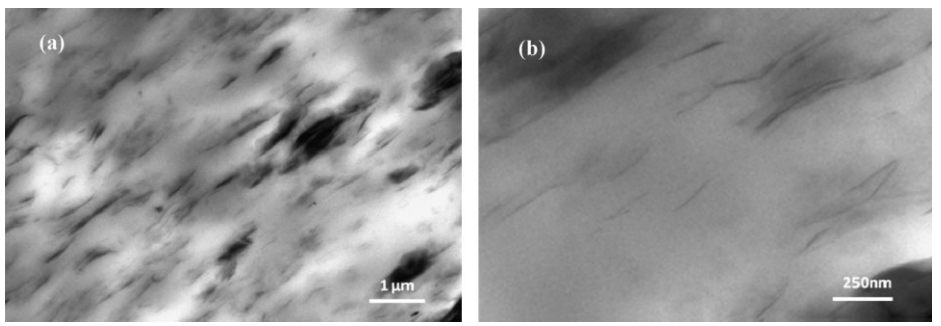

Figure 4.
TEM micrographs of the system containing cloisite at different magnifications: 12500X (a) and 60000X (b).

Effect on PP Crystallization

The influence of the addition of the nanofillers on PP crystallization was evaluated by means of XRD and DSC analysis.

In Figure 5 and 6 we report the XRD diffraction patterns of the spectrum portion related to PP crystalline phase.

Blank PP and PP + PPgMA show the typical XRD diffractogram of the monoclinic α phase of iPP. Occurrence of β-modification (2θ 16) is also observed which is common for commercial grades of meltcompounded iPP.[18]

Filled PP crystallizes with the same phase of the pristine polymer with however a significant variation of the intensity ratio between two XRD peaks (110 diffraction, peak I and 040 diffraction, peak II) in all composites. This can be attributed to a preferential growth of PP crystallites well ordered along the b direction.

These results are even more prominent if we consider the system containing C20A (Figure 6), for which the (040) orientation is such that all the other diffraction signals have almost the intensity of the background noise. Therefore this material is crystallizing almost only along the (040) direction, thus evidencing a very high degree of interaction with the filler.

The same effect on the α phase of PP was already reported in literature for PP composites filled with nanoparticles such as calcium phosphate, talc, pyrophyllite and organophilic clays (montmorillonite and attapulgite)[19–23].

Furthermore, the induction in PP of very ordered structures around the sepiolite (called mesophase or interphase), different from those in the unfilled matrix, was already observed[24,25] and a preferential PP orientation was found by our research group.[26]

We can therefore conclude that a strong interaction is established between the PP macromolecules and the fillers as they can strongly influence the crystallisation behaviour of the matrix. In particular we can observe that the ratio PeakI/PeakII decreases from F100 to Disperal/CD1 to C20A.

The crystallisation behaviour of the materials was further studied through DSC analysis in particular taking in to consideration the crystallisation temperature from the cooling scan and the degree of crystallinity calculated from the melting enthalpy of the first and second heating scan (Table 3).

For all the studied systems, with the exception of F100, we can identify an increase in the crystallisation temperature indicating a nucleation promotion played by the nanofillers; this being particularly evident in the case of C20A (+ 12 °C) and Disperal (+ 7 °C).

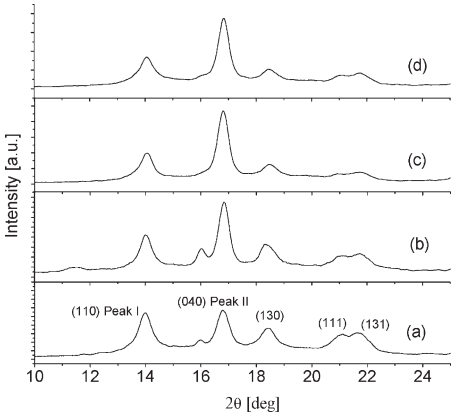

Figure 5.
XRD spectra, PP crystalline phase region, of PP (a), PP + F100 (b), PP + CD1 (c), PP + Disperal.

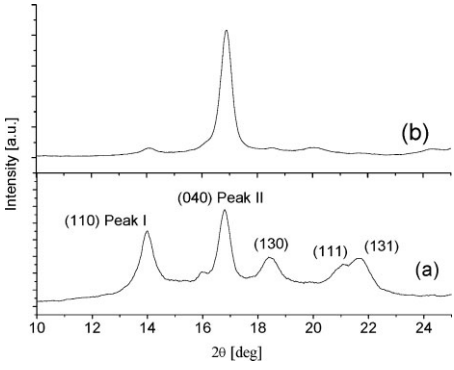

Figure 6.
XRD spectra, PP crystalline phase region, of PP + PPgMA (a), PP + PPgMA + C20A (b).

Table 3.
DSC Crystallinity data and crystallisation values.

SAMPLE	T_c(°C)	X_c(%) I scan	X_c(%) II scan
PP	115	53	64
PP + PPgMA	110	49	54
PP + PPgMA + C20A	122	52	62
PP + F100	114	54	65
PP + CD1	118	57	60
PP + Disperal	122	53	59

When we consider the matrix crystallinity we can evidence that the addition of the fillers has a scarce influence on the as-prepared specimens (first scan) whereas we can underline an increase of the degree of crystallisation upon addition of C20A ($\Delta X_c = 6\%$) as calculated from the DSC second scan. All the other systems have almost no influence.

Thermal Behaviour

The influence of nanofillers on the thermal degradation behaviour of PP was explored by means of TGA performed in inert and oxidising atmospheres; results are shown in Figure 7.

During heating under nitrogen, PP thermally degrades in a single step to volatile products above 350 °C ($T_{5\%}$ 416 °C, T_{max} 462 °C, Figure 7a) through a radical chain process propagated by carbon-centred radicals that arise from carbon–carbon bond scission.[27] A very similar behaviour is observed for PP + PPgMA (Table 4). In general the addition of nanofillers has a scarce influence on PP thermal degradation, with the exception of C20A and CD1; indeed upon the addition of these fillers, PP weight loss is anticipated, especially as far as T_{max} is concerned (Table 4).

This behaviour was already observed by Marcilla et al.[28] and by Tartaglione et al.[24] for sepiolites and attributed to a catalytic action, likely to happen with a mechanism similar to the catalytic thermal cracking of alkanes that occurs using zeolites.

An analogous catalytic effect was also reported by other authors for PP nanocomposites filled with lamellar layered organoclays in which, very similarly to what happens in the systems treated here, despite a slightly delayed thermal degradation in the early stage of weight loss, the main volatilization step was accelerated.[29] We must also underline that the material containing C20A degrades much faster than all the other systems, as can be recognised analysing the derivative weigh loss peak which is much sharper and higher in intensity than the others. The catalytic action of layered silicates on PP thermal degradation is confirmed by the fact that PP-fluorohectorite nanocomposites, in which acid silanols are absent being replaced by fluorine atoms, show a

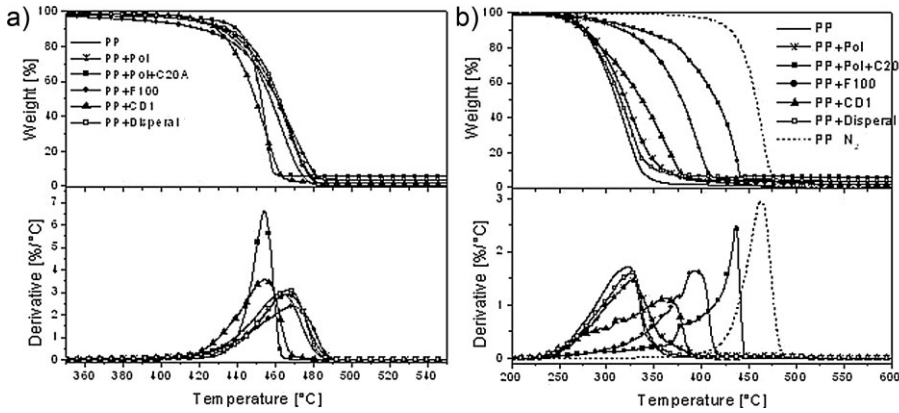

Figure 7.
TGA and differential thermogravimetric analysis (DTG) curves in nitrogen (a) and in air (b).

Table 4.
Degradation temperatures in nitrogen and in air.

Samples	$T_{5\%}$ N_2 (°C)	T_{max} N_2 (°C)	$T_{5\%}$ air (°C)	T_{max} air (°C)
PP	416	462	266	323
PP + PPgMA	416	466	268	327
PP + PPgMA + C20A	427	454	300	436
PP + CD1	420	454	260	362
PP + F100	389	469	291	393
PP + Disperal	417	467	262	327

stabilisation effect towards PP thermal degradation.[30]

In air, above 200 °C the radical chain thermal volatilization is initiated by H abstraction from PP by oxygen.[27] Volatilization begins in TGA below 270 °C ($T_{5\%}$), with T_{max} at 324 °C (solid line, Figure 7b and Table 4), and is completed before the temperature of the initiation of the pure thermal degradation process (400 °C) is reached (dotted line, Figure 7b). A very similar behaviour is observed for PP + PPgMA (Figure 7b and Table 4).

From Figure 7b we can clearly see that layered fillers play an important role in protecting PP from degradation by retarding both the weight loss onset and maximum degradation temperature, yet with noticeable differences between montmorillonites and hydrotalcites. Indeed F100 increases PP $T_{5\%}$ of about 25 °C and T_{max} of 70 °C whereas a much higher effect is noticed with C20A which shifts PP $T_{5\%}$ of from 266 to 300 °C and T_{max} from 323 to 436 °C (Table 4). It is worth noticing that by increasing PP T_{max} of more than 110 °C, C20A makes the polymer degrade at temperatures very close to those in nitrogen; in particular we can observe that at a temperature coincident with that of PP onset degradation in nitrogen ($T_{5\%}$, 416 °C) there is still a considerable amount of material to be degraded for the system containing C20A (*ca.* 50%) whereas the pure polymer concludes its degradation process at temperatures far below this one (*ca.* 375 °C).

Layered fillers are well known to protect polymeric materials from thermoxidative degradation by behaving as superior insulator and mass transport barrier to the volatile products generated during decomposition and to the oxygen from the gas phase to the polymer.[1] The higher efficiency of montmorillonite if compared to hydrotalcite can be associated to the former higher aspect ratio which promotes the formation of a more efficient superficial barrier layer.[31]

Another significant feature to be considered is the shape of the two derivative curves, which is in both cases extremely asymmetrical with respect to that of the pure polymer with very low rates at the beginning of the degradation and ending with a very high weight loss rate at higher temperatures. This is due to the fact that in the low temperature side of the derivative curves PP ablation gradually leads to formation of a surface ceramic barrier layer which partially screens oxygen, thus limiting the weight loss rate increase with temperature as compared to clay-free PP. The protecting action of the inorganic skin makes part of PP to survive until temperatures are reached (above 400 °C) at which thermally initiated carbon-carbon bonds scission becomes possible, thus contributing to volatilisation in addition to oxygen initiated degradation in the high temperature side of TGA derivative curves. This behaviour was already observed for PP systems containing carbon nanotubes.[32]

Also sepiolites partially protect PP from degradation by increasing T_{max} of about 40 °C; this was already observed in a previous work of ours and attributed both to the formation of a protective layer, as in the case of layered fillers, and to the sorptive properties of sepiolites towards volatiles and oxygen itself.[26] The lower stabilization effect brought by sepiolites

may be attributed to their shape factor (needle-like) which, by cumulation of the clay on the surface of degrading nanocomposite, leads to a less effective barrier than in the case of layered inorganics.

Disperal has almost no influence on the degradation pattern, this could be due to either the low level of dispersion/distribution or to the low aspect ratio.

Mechanical Properties

The mechanical properties of the prepared materials were addressed by means of tensile tests. The results are reported in Figure 8 and Table 5.

From a general point of view, the tensile modulus of a polymeric material has been shown to be remarkably improved when nanocomposites are formed with layered silicates.[2]

From Table 5 and Figure 8 it is clear that the fillers play different roles in influencing the mechanical properties of PP. Montmorillonite C20A increases to a large extent PP Young's modulus (ca. 76%) thereby significantly decreasing elongation at break and generating a fragile material. The same trend, even though at minor extent, can be observed for sepiolite CD1 with an increase of the Young's modulus of about 46% and a similar decrease in the elongation at break.

The increment in modulus is attributed to the reinforcing effect of dispersed nanofillers with high aspect ratio which act as efficient stress transfer agents, on the other hand the fragile behaviour is attributed to the fraction of poorly dispersed nanoparticles as determined by SEM and TEM observations.

Hydrotalcite F100 and Disperal have a negligible influence on Young's modulus values, in the first case this may be attributed to the lower strength and aspect ratio[31] and higher flexibility of the layers[33] with respect to montmorillonite and in the second case to the low aspect ratio and poor dispersion. Special attention must indeed be dedicated to the elongation at break as F100 limits its decrease with respect to the other fillers; this could be due to a limited plasticizing effect is provided by the C_{16}-C_{18} modifier present in F100.[34]

The differences encountered comparing the same filler typologies (silicates: montmorillonite C20A and sepiolite CD1) can be ascribed to the different aspect ratio that makes layered ones more suitable to provide a reinforcing effect, also taking into consideration the lower degree of

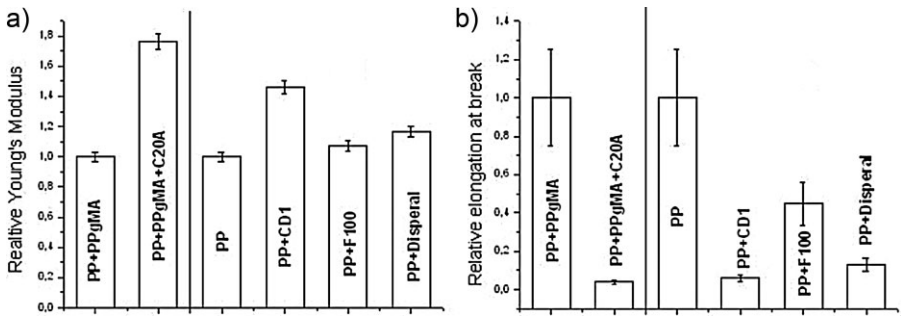

Figure 8.
relative Young's modulus (a) and elongation at break (b).

Table 5.
Mechanical performances.

Samples	PP	PP + PPgMA	PP + PPgMA + C20A	PP + CD1	PP + F100	PA6 + Disperal
E (MPa)	1570	1520	2680	2290	1680	1850
ε_b (%)	151.5	221.1	3.6	9.4	60.9	20.8

distribution of C20A evidenced by SEM analysis (Figure 2). It is worth noticing that the role plaid by C20A cannot be attributed to an increased PP crystallinity (Table 3, first scan data), which may account for an increased Young's modulus, but has to be strictly related to the reinforcing effect provided by the clay platelets.

It is therefore clear that, as far as mechanical properties are concerned, both dispersion and chemical nature of the filler play a fundamental role.

Combustion Behaviour

Combustion tests were performed by means of a cone calorimeter apparatus. Layered silicates and hydrotalcites are well-known to reduce the rate of combustion of polymeric materials.[1,35,36] In the case of montmorillonites, the nanocomposites' flame retardant mechanism involves a high-performance carbonaceous-silicate char, which builds up on the surface during burning. This insulates the underlying material and slows the mass loss rate of decomposition products.[37]

On the other hand, the flame retardant performances of hydrotalcite in micro-composites in the mass loss calorimeter were explained by the heat absorption related to the water loss over a wide temperature range.[35] The authors, in particular, compared by cone calorimeter the performances of hydrotalcites and boehmites microcomposites in poly-(ethylene-co-vynil acetate), the former being much more effective as flame a retardant, because of boehmite's lower water production and heat absorbed by the decomposition reaction.

For the systems studied in this paper, the heat release and mass curves as a function of time are reported in Figure 9 and some significant combustion values are reported in Table 6.

It is clear also in this case that the fillers act differently in protecting PP from combustion, the best performances in terms of HRR being obtained with montmorillonite C20A with a 60% reduction of pkHRR although no significant differences were encountered as far as total heat released is concerned (THR, Table 6). Good performances are also observed with hydrotalcite F100 with a pkHRR decrease of about 45%, CD1 and Disperal displaying a limited influence on pkHRR reductions (Figure 9a). The results showed for

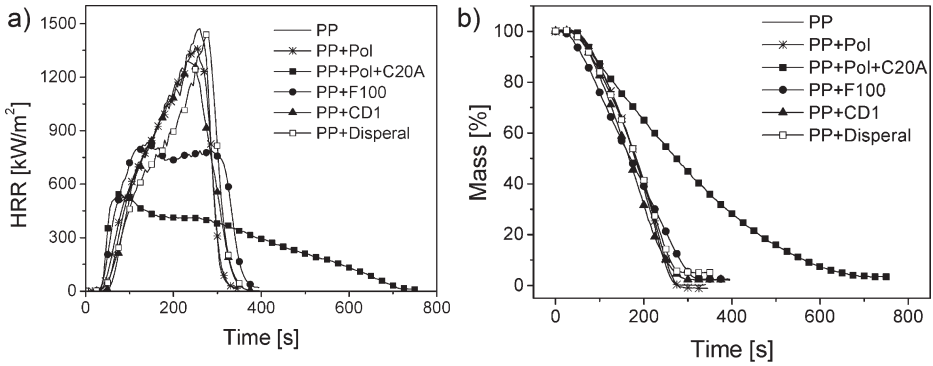

Figure 9.
Cone calorimeter curves. Heat Release Rate vs. time (a) and mass (normalized on initial weight) (b).

Table 6.
Cone Calorimeter results (percentage reduction with respect to matrix).

Samples	PP	PP + PPgMA	PP + PPgMA + C20A	PP + CD1	PP + F100	PP + Disperal
pkHRR (kW/m²)	1470 (–)	1365 (–)	545 (60)	1290 (12)	840 (42)	1440 (2)
THR (MJ/m²)	222 (–)	219 (–)	198 (9)	213 (4)	209 (6)	212 (4)

hydrotalcite 100 are well in line with what reported by Manzi-Nshuti et. al for PP systems without compatibiliser.[38]

The shape of the curve is also of major importance, developing from the one typical of non charring materials in which a steady HRR is only marked by a shoulder in the early stages of the burning process with a subsequent increase of HRR, to the one typical of thermally thick charring (residue forming) samples which shows an initial increase in HRR until an efficient char layer is formed and, as the char layer thickens, HRR decreases.[15] The former being observed in pristine PP and in the materials containing Dsiperal and sepiolite CD1 and the latter partially in that containing hydrotalcite F100 and in a more evident way in that containing montmorillonite C20A, in the latter case also accounting for an increase in the burning time from ca 300 sec to more than 700 sec.

The lower combustion rate for the system containing C20A resulted in an overall slower weight loss as compared to neat polymer (Figure 9b). On the other hand, the other systems do not present significant differences as far as the weight loss is concerned.

The mass loss rate, not shown here, follows the same trend of the heat release rate shown in Figure 9 with lower values for the systems containing F100 and C20A.

We believe that C20A and CD1 act in the same manner in protecting a polymeric material form combustion, *i.e.* through the formation of a superficial ceramic layer which prevents material from burning. It is therefore clear that layered fillers are in this case more effective in creating such layer.

As far as hydrotalcite F100 and Disperal are concerned, we have reported above that the water formation upon degradation is one of the key factors for their role as flame retardants;[35] apparently this feature does not allow F100 to influence PP combustion behaviour in the same manner as C20A, nevertheless its good dispersion, if compared to Disperal, makes it more efficient, dispersion being recognised as one of the key factors to allow a good flame retardant action of hydrotalcites.[39]

These statements are confirmed by analyzing the combustion residues (Figure 10) especially considering that PP and PP + PPgMA, not shown here, leave no residue at the end of the test.

The ability of a fire retardant to promote char formation upon combustion is one of the possible mechanisms of action of this class of materials. From Figure 10 it is

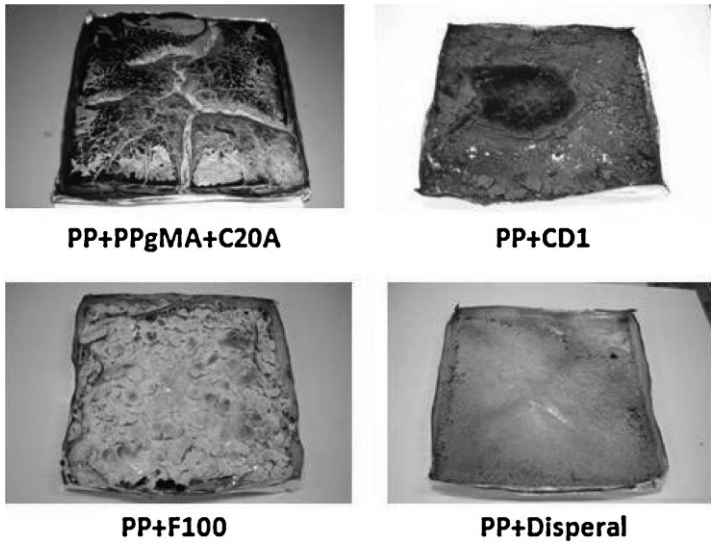

Figure 10.
Combustion tests residues.

therefore clear the reason why the best performing materials are, in this respect, layered silicates, due to the partial carbonization of the residue, as evident from the black spots present on the otherwise white ceramic structure. This feature is not present in the other systems, accounting for their lower efficiency. In particular for F100 the white residue left belongs only to the de-hydrated structure of the filler and therefore its flame retardant action can be ascribed to a combination of barrier provided by the ceramic layer and flame quenching due to water emission, without any char formation.

In a previous work of ours[40] we draw the same conclusions for PA6 based systems but in that case montmorillonite and organic hydrotalcite performances were very similar under cone calorimeter analysis. We can hypothesize that this can be due to the higher effect that water flame quenching has on PA6 rather than on PP combustion process. It is again clear that the possible mechanisms of action of the various fillers not only depend on the filler itself physical or chemical nature but also on the polymer base taken in to consideration.

The combustion residues of the materials containing F100 and Disperal are very similar, this confirming the fundamental role played by low-temperature dispersion on flame retardancy performances.

Conclusion

In this paper we evaluated the influence of nanofillers chemical nature, shape factor and organic modification on some selected PP characteristics, ranging from crystallinity (through XRD and DSC) to mechanical properties, to thermal resistance and, finally, combustion behaviour. The choice was to keep the same inorganic content in order to better evaluate the real influence of the above factors on the final material properties.

We evidenced that all aspects are important in determining the material performances. In particular, the low temperature properties, such as crystallinity and mechanical properties are strongly influenced by the inorganic nature and dispersion of the filler and by the chemical nature of the compatibiliser. Among natural fillers, montmorillonite C20A promotes PP chains orientation along the b direction and tends to increase material stiffness (higher Young's modulus). On the other hand, although scarcely influencing PP stiffness, probably because of the poor mechanical properties of the layers, and despite a good compatibility with the matrix, organically modified hydrotalcite F100 was found not to decrease to large extents its ductility due to the plasticizing effect of the C_{16}-C_{18} anion present in the interlayer.

The poor dispersion of Disperal in PP may account for its overall negligible influence on PP mechanical properties.

Both the chemical nature of the filler, its shape factor and the original (low temperature) dispersion were all found to play a key role as far as high temperature properties are concerned. In particular we observed that natural clays catalyze PP thermal degradation due to the catalytic action of acidic sites on the filler surface. The same is not observed for hydroxides, which have very poor influence, if any, on PP degradation mechanisms.

The addition of all fillers, with the exception of Disperal, was found to be beneficial in increasing the thermoxidative resistance of the polymer; the scarce influence of Disperal being ascribed, as for all other properties, to its poor dispersion in PP. On the other hand, among natural fillers, the best performances of C20A are attributed to its higher aspect ratio as compared to CD1; conversely, despite its higher aspect ratio and compatibility with PP, F100 has a lower protecting action as compared to C20A most probably because its lower mechanical resistance that makes the barrier protection less effective.

A combination of charring promotion and flame quenching makes F100 behave as an efficient flame retardant. The pkHRR

values obtained with this filler are nevertheless higher than those obtained with C20A, which is a more efficient char promoter (as determined by analyzing the residues after cone calorimeter tests) due to the well-known barrier mechanisms played by layered silicates during combustion. Layered silicates are also more efficient as flame retardants than needle-like ones due to their higher tendency to promote charring again probably because of the easiness to build up a homogeneous protective ceramic layer.

On the other hand, despite being able of flame quenching, due to water elimination during degradation, Disperal has almost no role as flame retardants because of the poor efficiency, which is a consequence of poor dispersion.

Acknowledgements: This study was carried out in the frame IP European research program "MULTIHYBRIDS", No. 026685-2, in the 6th Framework Program. The authors would like to thank Dr. Masarati and the Electronic Microscopy Laboratory from Lyondelbasell for TEM analysis.

[1] S. S. Ray, M. Okamoto, Polymer/layered silicate nanocomposites: a review from preparation to processing. *Prog. Polym. Sci.* **2003**, *28*, 1539–1641.
[2] D. R. Paul, L. M. Robeson, Polymer nanotechnology: nanocomposites. *Polymer* **2008**, *49*, 3187–3204.
[3] F. Hussain, M. Okamoto, R. E. Gorga, Polymer matrix nanocomposites, processing manufacturing and application: an overview, *J. Comp. Mater.* **2006**, *40*(17), 1511–1575.
[4] A. Okada, A. Usuki, Twenty years of polymer-clay nanocomposites. *Macromol. Mater. Eng.* **2006**, *291*(12), 1449–1476.
[5] J. H. Du, J. Bai, H. M. Cheng, The present status and key problems of carbon nanotube based polymer composites. *Express Polym. Lett.* **2007**, *1*(5), 253–273.
[6] G. Li, L. Wang, H. Ni, C. U. Pittman, Jr., Polyhedral Oligomeric Silsesquioxane (POSS) polymers and copolymers: a review. *J. Inorg. Organomet. Polym.* **2001**, *11*(3), 123–145.
[7] J. Buitenhuis, L. N. Donselaar, P. A. Buining, A. Stroobants, H. N. W. Lekkerkerker, Phase separation of mixtures of colloidal boehmite rods and flexible Polymer. *J. Colloid Interface Sci.* **1995**, *175*(1), 46–56.
[8] R. C. Streller, R. Thomann, O. Torno, R. Muelhaupt, Isotactic Poly(propylene) nanocomposites based upon boehmite nanofillers. *Macromol. Mater. Eng.* **2008**, *293*(3), 218–227.
[9] F. Leroux, J. P. Besse, Polymer interleaved Layered Double Hydroxide: a new emerging class of nanocomposites. *Chem. Mater.* **2001**, *13*, 3507–3515.
[10] D. H. Kim, P. D. Fasulo, W. R. Rodgers, D. R. Paul, Structure and properties of polypropylene-based nanocomposites: effect of PP-*g*-MA to organoclay ratio. *Polymer* **2007**, *48*(18), 5308–5323.
[11] K. H. Wang, M. Xu, Y. S. Choi, I. J. Chung, Effect of aspect ratio of clay on melt extensional process of maleated polyethylene/clay nanocomposites. *Polym. Bull.* **2001**, *46*, 499–505.
[12] Y. Dong, D. Bhattacharyya, Effects of clay type, clay/compatibiliser content and matrix viscosity on the mechanical properties of polypropylene/organoclay nanocomposites. *Composites Part A* **2008**, *39*(7), 1177–1191.
[13] E. Bilotti, H. R. Fischer, T. Peijs, Polymer nanocomposites based on needle-like Sepiolite clays: effect of functionalized polymers on the dispersion of nanofiller, crystallinity, and mechanical properties. *J. Appl. Polym. Sci.* **2008**, *107*, 1116–1123.
[14] E. P. Moore, *Polypropylene Handbook*, Cincinnati Hansen/Gardner, 1996.
[15] B. Schartel, T. R. Hull, Development of fire-retarded materials - Interpretation of cone calorimeter data. *Fire. Mater.* **2007**, *31*(5), 327–354.
[16] H. S. Lee, P. D. Fasulo, W. R. Rodgers, D. R. Paul, TPO based nanocomposites. Part 1. Morphology and mechanical properties. *Polymer* **2005**, *46*(25), 11673–11689.
[17] U. Costantino, A. Gallipoli, M. Nocchetti, G. Camino, F. Bellucci, A. Frache, New nanocomposites constituted of polyethylene and organically modified ZnAl-hydrotalcites. *Polym. Degrad. Stab.* **2005**, *90*, 586–590.
[18] J. Varga, G. W. Ehrenstein, Beta-Modification of Isotatic Polypropylene. In: J. Karger-Kocsis, (Ed.), *Polypropylene: An A-Z Reference*, London Kluwer Academic Publishers, 1999.
[19] E. Ferrage, F. Martin, A. Boudet, S. Petit, G. Fourty, F. Jouffret, P. Micoud, P. De Parseval, S. Salvi, C. Bourgerette, J. Ferret, Y. Saint-Gerard, S. Buratto, J. P. Fortune, Talc as nucleating agent of polypropylene: morphology induced by lamellar particles addition and interface mineral-matrix modelization. *J. Mater. Sci.* **2002**, *37*, 1561–1573.
[20] B. Kim, S. H. Lee, D. Lee, B. Ha, J. Park, K. Char, Crystallization kinetics of maleated polypropylene/clay hybrids. *Ind. Eng. Chem. Res.* **2004**, *43*, 6082–6089.
[21] S. Radhakrishnan, P. Sonawane, N. Pawaskar, Effect of thermal conductivity and heat transfer on crystallization, structure, and morphology of polypropylene containing different fillers. *J. Polym. Sci.* **2004**, *93*, 615–623.

[22] C. Saujanya, S. Radhakrishnan, Structure development and crystallization behaviour of PP/nanoparticulate composite. *Polymer* **2001**, *42*(16), 6723–6731.
[23] L. Wang, J. Sheng, Preparation and properties of polypropylene/org-attapulgite nanocomposites. *Polymer* **2005**, *46*(16), 6243–6249.
[24] A. Linares, E. Morales, M. C. Ojeda, J. L. Acosta, Interphase in polypropylene-sepiolite composites based on dynamic mechanical analysis. *Die Angewandte Makromolekulare Chemie* **1987**, *147*(1), 41–47.
[25] J. L. Acosta, E. Morales, M. C. Ojeda, A. Linares, Effect of addition of sepiolite on the mechanical properties of glass fiber reinforced polypropylene. *Die Angewandte Makromolekulare Chemie* **1986**, *138*(1), 103–110.
[26] G. Tartaglione, D. Tabuani, G. Camino, M. Moisio, PP and PBT composites filled with sepiolite: morphology and thermal behaviour. *Compos. Sci. Technol.* **2008**, *68*, 451–460.
[27] N. Grassie, G. Scott, *Polymer degradation and stabilization*, Cambridge Cambridge University Press, 1985.
[28] A. Marcilla, A. Gomez, S. Menargues, R. Ruiz, Pyrolysis of polymers in the presence of a commercial clay. *Polym. Degrad. Stab.* **2005**, *88*, 456–460.
[29] W. Gianelli, G. Ferrara, G. Camino, G. Pellegatti, J. Rosenthal, R. C. Trombini, Effect of matrix features on polypropylene layered silicate nanocomposites. *Polymer* **2005**, *46*(18), 7037–7046.
[30] M. Zanetti, G. Camino, P. Reichert, R. Muelhaupt, Thermal behaviour of poly(propylene) layered silicate nanocomposites. *Macromol. Rapid Commun.* **2001**, *22*, 176–180.
[31] L. A. Utracki, M. Sepehr, E. Boccaleri, Synthetic, layered nano-particles for PNC. *Polym. Adv. Technol.* **2007**, *18*, 1–65.
[32] D. Tabuani, W. Gianelli, G. Camino, M. Claes, Polypropylene based carbon nanotubes composites: structure and properties. *E-polymers* **2007**, 103.
[33] M. Ardanuy, J. I. Velasco, M. Antunes, M. A. Rodriguez-Perez, J. A. de Saja, Structure and Properties of Polypropylene/Hydrotalcite Nanocomposites. *Polym. Comp.* **2009**, 10.1002/pc.20869
[34] H. B. Hsueh, C. Y. Chen, Preparation and properties of LDHs/epoxy nanocomposites. *Polymer* **2003**, *44*, 5275–5283.
[35] G. Camino, A. Maffezzoli, M. Braglia, M. De Lazzaro, M. Zammarano, Effect of hydroxides and hydroxycarbonate structure on fire retardant effectiveness and mechanical properties in ethylene-vinyl acetate copolymer. *Polym. Degrad. Stab.* **2001**, *74*, 457–464.
[36] A. Castrovinci, G. Camino, Fire-Retardant Mechanisms in Polymer Nano-Composite Materials In: S. Duquesne,, C. Magniez,, G. Camino, Eds., *Multifunctional Barriers for Flexible Structure Textile, Leather and Paper*, Berlin Heidelberg Springer-Verlag, 2007, 87–108
[37] J. W. Gilman, Flammability and thermal stability studies of polymer layered-silicate (clay) nanocomposites. *Appl. Clay. Sci.* **1999**, *15*(1–2), 31–49.
[38] C. Manzi-Nshuti, P. Songtipya, E. Manias, M. Jimenez-Gasco, J. M. Hossenlopp, C. A. Wilkie, Polymer nanocomposites using zinc aluminum and magnesium aluminum oleate layered double hydroxides: Effects of the polymeric compatibilizer and of composition on the thermal and fire properties of PP/LDH nanocomposites. *Polym. Degrad. Stab.* **2009**, *94*, 2042–2054.
[39] C. Nyambo, D. Chen, S. Su, C. A. Wilkie, Does organic modification of layered double hydroxides improve the fire performance of PMMA? *Polym. Degrad. Stab.* **2009**, *94*, 1298–1306.
[40] D. Tabuani, S. Ceccia, G. Camino, Nylon-6 nanocomposites, study of the influence of the nanofiller nature on morphology and material properties. *J. Pol. Sci. Part B* **2009**, *47*, 1935–1948.

